FULL PAPER

Fouling Characteristics and Electrochemical Recovery of Carbon Nanotube Membranes

*Xinghua Sun, Ji Wu, Zhiqiang Chen, Xin Su, and Bruce J. Hinds**

The fouling behavior of carbon nanotube (CNT) membranes is investigated for large protein biomolecules and a wide variety of small molecules. The CNT membranes are largely fouling resistant, even to untreated river water, due to size exclusion and an inert graphitic core that supports fast fluid flow. However, it is found that bovine serum albumin (BSA) and naphthalene significantly foul membranes due to solution coagulation and π–π stacking, respectively. Small single-walled (SW) CNTs (<1.5 nm i.d.) are difficult to foul with BSA when precipitation is prevented, showing that size exclusion at SWCNT tips can prevent fouling. Electrochemical oxidation, bubble generation and ionic pumping are shown to recover membrane performance. Electrochemical oxidation at greater than +1.4 V is seen to oxidize CNTs as well as biofoulants, but H_2 bubble generation at –2 V lifts foulants without damage to the membrane allowing for repeated cycles. Ionic pumping using large cations is seen to remove small molecule foulants adsorbed to the CNT core. The relatively narrow class of foulants and three complementary methods of membrane defouling make the CNT membrane platform a potentially robust system for a wide variety of chemical separations and environmental water treatments.

1. Introduction

Nanoporous membranes play critical roles in bioseparations, water purification, drug delivery and biosensing, benefiting from high selectivity and high throughput that is associated with continuous processes.[1] However, membrane fouling still remains the most difficult challenge for long-term use and much effort is focused on membrane regeneration cycles such as chemical clean and reverse flow cycles.[2] Carbon nanotube (CNT) membranes are an emerging material system with unique properties such as high permeability to water and have inherent electric conductivity. The smooth graphitic cores of CNT membranes make them possible to allow dramatic enhancements in flow velocity of 10 000 fold compared to conventional pores.[3] Functional chemistry can be placed at CNT tips to give "gatekeeper" separations that mimic the performance of protein channels,[4] and applied bias can induce dramatic ion-induced fluid flow.[5] Promising applications of CNT membranes have been demonstrated in water purification,[6] drug delivery[7] and bioseparations.[8] However, there has not been a dedicated investigation about CNT membrane fouling and defouling, which is a critically practical issue for separation applications containing biological foulants or small molecule adsorbents. It is necessary to survey potential foulants of the CNT membrane system and what methods can be used to regenerate flow performance.

Four key fouling mechanisms of conventional membranes are commonly accepted: complete pore blockage, intermediate pore blockage, pore constriction and cake filtration.[9] On the basis of the specific mechanisms, antifouling or defouling strategies can be developed. These consist of numerous physical and chemical methods such as surface chemical treatments or reverse flow cycles. For the CNT membrane system, we expect the primary fouling mechanisms to be: 1) tip coordination, 2) π–π stacking or hydrophobic binding within CNT core, and 3) caking on the top surface. In the case of tip coordination, the tip chemistry can be modified to be selective to target permeate and the small size of CNTs can give size exclusion to larger molecules. In the case of π–π stacking, the atomically flat surfaces that support fast fluid flow should also allow adsorbates to flow along the CNT surface.[10] In the case of caking, more traditional methods can be explored. However, it must be pointed out that CNT membranes are different from commercial membranes, in that conductive CNTs embedded in an insulating polymer can give highly localized electric field for electrochemical reactions[11] and ionic pumping.[5a,b] For instance, CNTs can be oxidized at voltages of +1 V to +1.7 V to reduce CNT lengths[3,8,12] and potentially oxidize organic foulants. Another promising approach to defouling cake layers or large protein foulants is based on bubble generation[13] by the electrochemical reduction of water at the tips of CNTs. For small molecule adsorption by π–π stacking or hydrophobic interactions it is possible to take advantage of the use of a large cation, $Ru(bpy)_3^{2+}$ (≈1 nm in diameter) that is accelerated under an applied electric field to

Dr. X. Sun,[+] Prof. J. Wu,[++] Z. Chen, X. Su,
Prof. B. J. Hinds
Department of Chemical and Materials Engineering
University of Kentucky
Lexington, KY 40506, USA
E-mail: bjhinds@engr.uky.edu
[+]Present address: Department of Bioengineering
University of Louisville, KY 40292, USA
[++]Present address: Department of Chemistry, Georgia Southern University, GA 30460, USA

DOI: 10.1002/adfm.201201265

potentially clean the inner core of nanotubes acting as a molecular brush.

In this report, we assay a large number of potential foulants for three types of lab-prepared CNT membranes, from large biomolecules to small molecule aromatics, using changes in transmembrane current. It is found that bovine serum albumin (BSA) and naphthalene significantly foul membranes due to solution coagulation and π–π stacking, respectively. Small single-walled (SW) CNTs (<1.5 nm inner diameter (i.d.)) are not fouled with BSA when precipitation is curtailed, showing size exclusion at nanometer-scale CNT tips can prevent fouling while larger multi-walled (MW) CNT membrane fouling by BSA was prevalent. Other common foulants, as well as untreated Kentucky River water, show no effect on double-walled (DW) CNT membrane. Electrochemical oxidation, bubble generation and ionic pumping are shown to recover membrane performance.

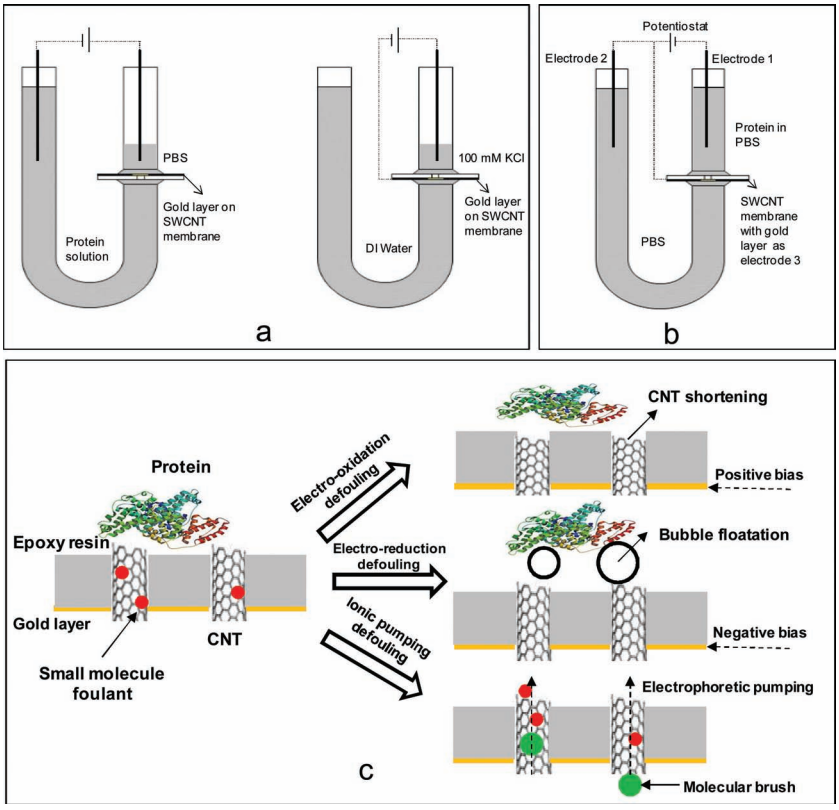

Figure 1. Membrane modules for fouling studies of CNT membranes and schematic of electrochemical defouling methods. a) Face-down fouling and face-up electrochemical defouling and trans-membrane ionic current measurements. b) Face up fouling and defouling. c) Schematic of mechanisms of defouling by electro-oxidation, electro-reduction or ionic pumping. The black line on the membrane between the o-rings represents gold contact and the white represents polycarbonate support with the membrane spanning a 3 mm diameter hole.

2. Results and Discussion

Large biomolecule fouling is the most prevalent cause of membrane performance loss. For this CNT fouling study, we first used BSA as a typical protein analog with 7.2 nm hydrodynamic diameter and negative charge at neutral pH. Fouling and defouling were carried out in different U-tube and electrode configurations designed to simulate different membrane processes (**Figure 1**). With the lower side of membrane facing the protein feed (Figure 1a), less membrane fouling was expected with weak large coagulants settling to the membrane surface. After fouling the U-tube was disassembled to test ionic current and the extent of fouling. In comparison, with the upper side of membrane facing the protein feed (Figure 1b), fouling would be more pronounced due to large protein coagulations on the membrane surface partially resulting in cake layer formation. The extent of fouling is then characterized by measuring the transmembrane ionic current of phosphate buffered saline (PBS) from Pt-electrode 1 (counter) and Pt-electrode 2. The configuration of Figure 1b more accurately depicts an operational geometry, where the membrane is not disassembled nor solutions exchanged therefore can be directly used to electrochemically oxidize CNT/foulant or generate bubbles during operation (CNT membrane used as working eletrode). During the fouling process, the negatively charged BSA is electrically pulled to the membrane surface with positive bias on the lower electrode. Considering the <1.5 nm i.d. pore of SWCNT membrane and 7.2 nm hydrodynamic diameter of BSA, transport of protein through CNT core is not expected but can partially block the CNT tip under electrophoretic driving force.[8] Therefore, pore blockage (complete or intermediate) and cake formation both exist in the configuration of Figure 1b, while CNT tip blockage would be the dominate mechanism in Figure 1a.

For the fouling experiment of a SWCNT membrane (Figure 1a), the ionic conductance decreased by around 20% compared with its original value after 48 h fouling (**Figure 2**). This is attributed to BSA or its aggregates blocking pore entrances (Figure 1c). The fouling extent characterized by the percentage of current drop was usually 15–35% for this membrane module and fouling process for 48 h. In contrast, dramatic fouling was observed upward facing SWCNT membranes (Figure 1b) with ≈90% fouling after 48 h (**Figure 3**). This is consistent with BSA aggregates gravity settling onto the membrane surface with a cake layer resulting in stronger blockage of the membrane.

Defouling of the SWCNT membrane was achieved by applying oxidation or reduction bias to the membrane as a working electrode. Figure 2 shows the oxidation voltage dependence of defouling efficiency using the experimental configuration of Figure 1a. Defouling was not seen when the oxidation bias was less than 0.8 V while partial defouling was obtained at the bias of +1.2 V. A bias of +1.4 V saw a slight (<10%) increase in transmembrane ionic current. Two possible defouling mechanisms are attributed to the oxidative defouling: oxidation of adsorbed protein and the electrochemical etching of the CNT itself. Cysteine, tyrosine and tryptophan of BSA can be oxidized

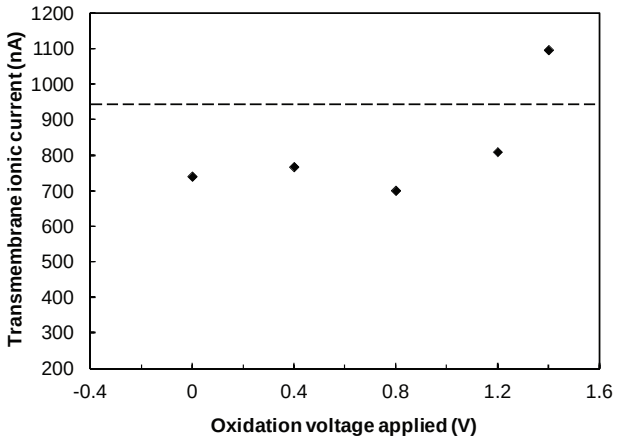

Figure 2. Effect of electrochemical oxidation voltage on an ionic current SWCNT membrane fouled by BSA with the experimental geometry depicted in Figure 1a. After fouling, the apparatus was re-assembled in the conformation shown in the second part of Figure 1a. Transmembrane ionic current was measured in 100 mM KCl solution at +0.6 V and the electrochemical oxidation defouling time was 20 min at each bias starting at +0.4 V. Initial membrane current was 946 nA (dashed line).

at the potential of +0.5, +0.7, and +0.8 V (vs Ag/AgCl), respectively.[14] The increase in transmembrane current after 1.7 V treatment is consistent with oxidation of CNTs reducing the path length through the membrane[8] which would have a limited number of cycles in practical applications.

Defouling of CNT membranes by electrochemical reduction of water to form H_2 bubbles is a unique approach enabled by conductive CNTs in insulating polymer matrix. Figure 3 showed that the transmembrane ionic current of BSA-fouled SWCNT membrane was mostly recovered by 10 min reduction treatment at the bias of –2 V in upward facing configuration of Figure 1b.

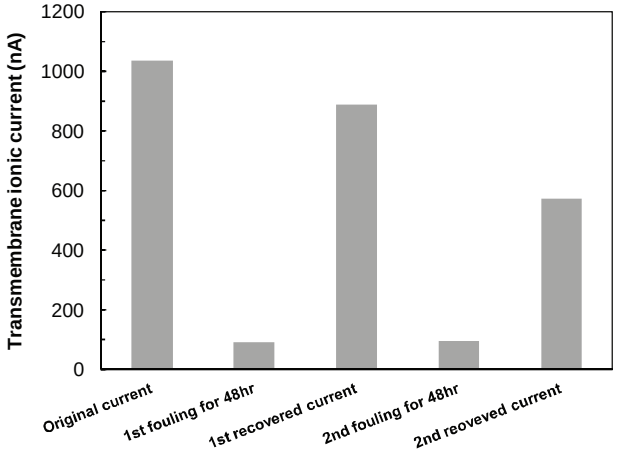

Figure 3. Sequential fouling and defouling of a SWCNT membrane with an upward facing membrane configuration (Figure 1b). The electrophoresis voltage was +1 V to foul membrane with BSA and gravity settling of coagulants. The transmembrane ionic current was measured using PBS (150 mM NaCl) and the electrochemical reductive defouling voltage and time were –2 V and 10 min, respectively.

Table 1. Comparison of sequential fouling and defouling of SWCNT and MWCNT membranes by BSA in vertically mounted fouling/defouling experiments. Fouling was induced by a +1 V electrophoretic driving force bias. Reduction defouling by bubble generation was performed at –2 V bias for 10 min.

Sequential fouling time		48 h	96 h	144 h
SWCNT membrane	Fouling	Negligible	Negligible	20.0%
	Defouling by reduction	N/A	N/A	Total current recovery
MWCNT membrane	Fouling	33.3%	19.0%	24.2%
	Defouling by reduction	Total current recovery	93.2%	Total current recovery

At the highest fouling face up configuration, the defouling efficiency was as high as 85% for the first fouling cycle, and 60% for the second cycle. This is consistent with reports that surface-active molecules such proteins can be concentrated around the gas-water interface of lifting bubbles[15] though more subtle denaturing effects may be present.[16]

In a prior BSA/lysozyme separation study in larger MWCNTs,[8] it was found that electrophoretically driven BSA was strong foulant since it could partially fit in the ≈7 nm i.d. CNT entrances and cores. However, the potential exists for BSA to not fit inside the much smaller SWCNT (≈1.5 nm i.d.). To test this hypothesis without forming a gravity-settled cake layer we used configuration similar to Figure 1b, except having the membrane mounted vertically at the bottom of the U-tube. SWCNT and MWCNT membrane fouling comparison is shown in **Table 1**. Fouling of the SWCNT membrane was negligible compared to the MWCNT membrane. This has important implications for water purification or desalination with SWCNT membranes in that large biomolecules do not fit into CNT pores and are not significant foulants unless a cake layer forms by protein aggregation, as seen in the 144 h run. Different from the fouling experiments with 3 cm H_2O pressure (Figure 1a), there no pressure was applied for the electrophoresis fouling using this vertical membrane setup. In both cases a reductive bubble generation treatment is able to give complete recovery. It should also be noted that the vertical mounting of membrane prevented fast cake formation caused by large protein aggregations as discussed on serious fouling setup (Figure 1b).

Both electrochemical oxidation and reduction are able to defoul large biomolecules, however a significant increase in flux was seen for oxidation case at much higher bias presumably due to the shortening of the CNT path length. For a periodic defouling process one would not want to permanently damage CNT membranes and it is expected that the reduction cycle would be preferred. To directly observe the length change of SWCNTs, UV-vis spectra and scanning electron microscopy (SEM) of SWCNT membranes were compared before and after electrochemical treatments. This experiment has the bottom side of membrane have CNTs that electrically contacted with gold layer while the top side is exposed for the electrochemical oxidation of CNTs which is similar to the operational geometry. **Figure 4** shows the UV-vis absorbance after oxidation at the voltage of +1.4 V or +1.7 V with a marked drop (11 ± 3%) in UV-vis absorbance after oxidation at +1.7 V for 5 h. The epoxy

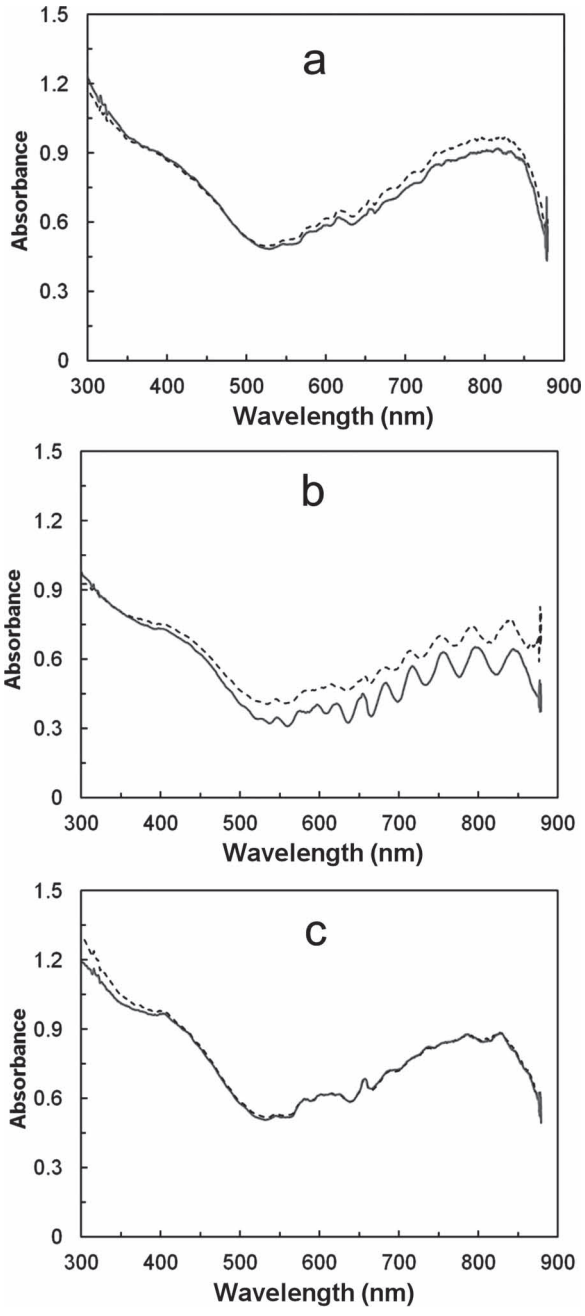

Figure 4. UV-vis absorbance comparison of SWCNT membranes with no protein before and after electrochemical treatments of oxidation at: a) +1.4 V for 5 h, b) +1.7 V for 5 h, and reduction at c) –2 V for 30 min. Dashed and solid lines represent absorbance before and after treatment, respectively.

matrix of the membrane is negligibly absorbing while CNTs are strongly absorbing in the visible range, thus the change in absorbance is proportional to a reduction in the length of CNTs (500 nm for the 5-μm-thick membrane). The drop was significantly less (4.7 ± 3%) after oxidation at +1.4 V for 5 h, indicating a milder condition for the periodic defouling of SWCNT membranes. For the reduction case, there is no expected electrochemistry with the carbon in the reduced state, and the

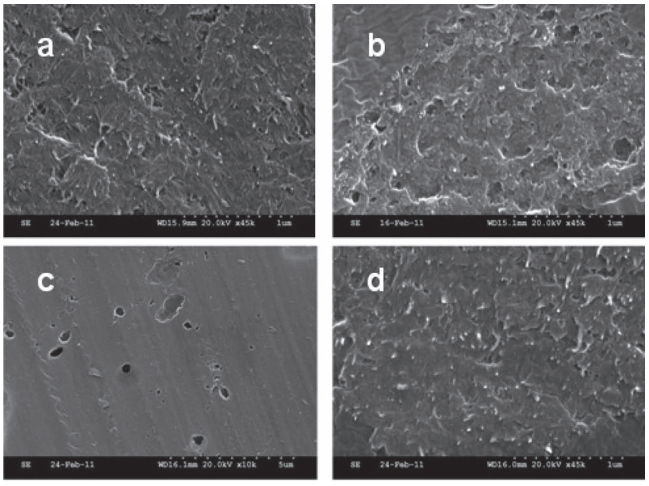

Figure 5. SEM top-view images of SWCNT membranes. a) As-made SWCNT membrane. b) After 5 h electrochemical oxidation at +1.4 V applied to the membrane working electrode. c) After 5 h electrochemical oxidation at +1.7 V. d) After 30 min electrochemical reduction at –2 V.

absorbance change after reduction treatment was negligible within the measurement uncertainty. Thus, the reduction treatment would be the preferred periodic defouling cycle for biomolecules on CNT membranes. It should be noted that the reduction treatment time (30 min) was shorter than the oxidation time (5 h) since a large amount of generated bubbles would cover the sample and make long term studies incomparable. The electron microscopy characterization of membranes before and after electrochemical treatment was consistent with UV-vis observations. The SEM image (**Figure 5**a) shows many CNT tips protruding from the surface after the microtoming process that forms the CNT membrane. After oxidation treatment at +1.7 V (Figure 5c) the tips are no longer visible and holes are formed, indicating CNT oxidation as the primary defouling mechanism. In comparison, treatment at +1.4 V (Figure 5b) shows only modest membrane damage that is consistent with the low defouling efficiency. This sacrificial process would have a limited number of cycles in use. The reduction reaction at –2.0 V shows that the CNT tips are intact, thus H_2 generation is the preferred operational method of biomolecule defouling.

Small molecule fouling is also of critical importance for CNT membrane use in water treatment, since real-world feed sources will have a mixture of large biomolecules and small organic molecules. In particular, it is expected that small aromatic molecules will have strong π–π interactions with CNT cores and thus foul the membrane. However, the atomically smooth graphite cores that support fast fluid flows should allow the adsorbate to be pushed out of the CNT and flow recovered. Also of interest is to see whether a wide variety of chemical species and common water foulants such as polymerizable humic acid or untreated river water will strongly foul CNT membranes. The DWCNT membranes with inner pore size between that of the SWCNT and MWCNT membranes were tested using various solutions, including pyrene butylic acid, naphthalene, rhodamine B, direct blue dye 71, Kentucky River water, BSA, alginic acid, humic acid, and toluene. As shown in **Table 2**, in the case of pyrene butylic acid, the transmembrane

Table 2. Summary of DWCNT membrane fouling and recovery using ionic current pumping of $Ru(bipy)_3^{2+}$. Percent current is calculated using the original current value. For the pyrene butylic acid study, the SWCNT membrane was used.

Reagent	Concentration [mg/mL]	Fouling time [h]	Defouling time [h]	Original current [A]	Current after fouling [A]	Current after defouling [A]
Pyrene butylic acid	0.7	18	15.4	5.7×10^{-06}	3.4×10^{-06} [60%]	6.5×10^{-06} [114%]
Naphthalene	10	20	23	8.9×10^{-07}	1.0×10^{-07} [11%]	1.8×10^{-07} [20%]
Rhodamine B	10	20	11	2.6×10^{-07}	1.3×10^{-07} [50%]	3.4×10^{-07} [131%]
Direct Blue Dye 71	10	72	N/A	2.2×10^{-06}	2.3×10^{-06} [105%]	N/A
Kentucky River water (without pressure)	N/A	20	N/A	2.3×10^{-06}	2.4×10^{-06} [104%]	N/A
Kentucky River water (with pressure)	N/A	96	N/A	5.4×10^{-07}	6.4×10^{-07} [119%]	N/A
Bovine serum albumin	10	96	22	8.9×10^{-07}	6.0×10^{-07} [67%]	6.2×10^{-07} [70%]
Alginic acid (pH 7)	10	18	N/A	6.4×10^{-07}	7.2×10^{-07} [113%]	N/A
Humic acid (pH 7)	10	120	N/A	7.2×10^{-07}	7.7×10^{-07} [107%]	N/A
Toluene	10	144	N/A	7.7×10^{-07}	7.0×10^{-07} [91%]	N/A

ionic current dropped by almost 40% due to the strong π-π interaction between the tube walls and the aromatic molecules. After cleaning using $Ru(bpy)_3^{2+}$, the ionic current was recovered completely since the large Ru cationic complex can function as a molecular brush. This supports the hypothesis that adsorbed small molecules can be pushed out of the CNT core with the atomically smooth surfaces. Although pyrene butylic acid is aromatic, it does have charge and is thus water soluble. For naphthalene, the ionic current was significantly reduced by more than 80% due to much more favorable partitioning to CNT surface and strong π–π stacking. The cleaning process with large cation is unable to recover transmembrane current, indicating a permanent fouling. In the case of toluene, a small aromatic molecule with a methyl group to prevent π–π stacking, only slight fouling of the membrane is observed. Rhodamine B is a positively charged ion that can interact with negatively charged carboxyl groups at the tip entrance of the membrane via Columbic electrostatic interaction, leading to the fouling of membrane (50% drop in ionic current). However, this weak electrostatic interaction can be easily removed by flushing the pores using big cations $Ru(bpy)_3^{2+}$. Direct Blue Dye 71 is a highly aromatic and negatively charged molecule (4 sulfonate groups per dye molecule). The highly charged and water soluble nature of this molecule resulted in no observation of π–π stacking-based fouling and did not coordinate to the anionic CNT tip. Of remarkable interest is that untreated Kentucky River water did not foul the membrane, despite many potential fouling reagents being present in the water source. In the water treatment community it is well known that alginic acid (pH 7) and humic acid (pH 7) are strong foulants, but we do not observe fouling with concentrated solutions, presumably do to the inert and hydrophobic nature of the CNT cores. BSA can nearly permanently foul the DWCNT membrane by more than 30%. Flushing using large cations is not an effective way to recover the original flux of the membrane. Considering the size of BSA is ≈7.2 nm, it is unable to enter the nanotube pore and block the mass transport. Again in this case, BSA forms a cake layer on the top of the epoxy film, resulting in the ionic current drop. This cake layer cannot be removed via molecular flushing which appears to be only effective when foulants are inside the nanometer-scale channels. However, as previously mentioned, generating H_2 nanobubbles is more effective at regenerating CNT membranes with large biomolecular layers at CNT entrances.

Due to low porosities of the microtome synthesized CNT membranes we were not able to directly measure pressure driven water flow. There is the clear relationship that reduced pore area will reduce fluid flow, however the exact relationship is not shown here. It is possible that flow rate may be reduced more than linearly since the fast fluid flow through CNTs is based on the atomic smoothness of graphite. For instance, a systematic study of functionalized CNT tips reduced flow through CNT tips by 100-fold[5c]. In this report, we cannot discern if all tips are partially blocked or a fraction of pores is completely blocked (only a linear reduction in flow). However, numerous applications of CNT membranes[4b] are based on gated diffusion or electrophoretic pumping that directly apply to this study. Charged foulant might affect the observed current nonproportionality to the pore area but at ionic strengths above 30 mM, the anions at CNT entrances were screened and bulk mobility was seen. In an another report,[17] charged CNT entrances showed rectification with small ions giving current with only one polarity. In this paper, high 100 mM concentrations were used and no rectification was seen, indicating that charge was not dominant in the fouling mechanism. It is also worth pointing out that the worst foulants were neutral (and aromatic) or the coagulation of BSA, as evidenced by the vertical mounting of the membrane to minimize BSA fouling). Thus, we expected a close relationship between the measured ionic current and the membrane pore area in this report.

3. Conclusions

Carbon nanotube membranes are resistant to fouling for a large class of molecules, including untreated Kentucky River water.

However, concentrated protein solutions (BSA) and π–π stacking aromatics (naphthalene) are seen to significantly foul the membrane. In the case of proteins, caking is the primary fouling mechanism and can be minimized by membrane geometry to avoid gravity settling and coagulation conditions. The smaller SWCNTs are less susceptible than MWCNTs to BSA fouling due to size exclusion, which is an important consideration for water treatment applications. Both electrochemical oxidation and reduction on CNT membrane electrodes efficiently defoul CNT membranes from biomolecule foulants. The oxidative treatment at voltages above 1.4 V, permanently etches CNTs, thus the reduction method to produce H_2 bubbles is the preferred method for frequent CNT membrane regeneration. Oxidation can be used for a limited number of cycles to remove strongly adsorbed foulants. However, that would also destroy any "gatekeeper" chemistry at CNT tips limiting an important method of separation. The CNT core is generally inert to fouling from small molecules. Since the CNT core is nearly atomically flat, adsorbed molecules can be pushed through the CNT core by the electrophoretic flow of large cations, thereby regenerating CNT membranes. The relatively narrow class of foulants and three complementary methods of membrane defouling make the CNT membrane platform a potentially robust system for a wide variety of chemical separations and environmental treatments.

4. Experimental Section

Chemicals: Dodecylbenzenesulfonic acid sodium and Triton-X 100 were purchased from Sigma. Polytetrafluoroethene (PTFE) membranes were from Sterlitech Corp. Epon 862 epoxy resin, hardener methylhexahydrophthalic anhydride, and catalyst 1-cyanoethyl-2-ethyl-4-methylimidazole were purchased from Miller Stephenson Chem. Co., Broadview Tech. Inc., and Shikoku Chemical, Japan, respectively. Pyrene butylic acid (Aldrich), naphthalene (Fluka), rhodamine B (Sigma), direct blue dye 71 (Sigma), bovine serum albumin (Sigma), alginic acid (Aldrich), humic acid (Aldrich) and toluene (PHARMACO AAPER) were used without purification. Kentucky River water was collected from Frankfort, Kentucky, USA.

CNT Membrane Fabrication: SWCNTs with a nominal inner diameter of 0.8–1.5 nm were purchased from Cheap Tubes and DWCNTs whose inner diameters range from 1.3 to 5 nm were purchased from Sigma Aldrich. MWCNTs were fabricated via a chemical vapor deposition on quartz substrate using ferrocene/xylene as the source gas and had an average outer diameter of 40 nm and an inner diameter of ≈7 nm.[18] CNT membranes were fabricated by the microtome-cut method,[19] modified for high CNT loading.[7] Briefly, 2.5 wt% CNTs were mixed with Epon 862 epoxy resin (Miller Stephenson Chem.) and Triton-X 100 (Sigma Aldrich). Methylhexahydrophthalic anhydride (MHHPA, Broadview Tech.) was used as a hardener. A Thinky centrifugal sheer mixer was used to thoroughly mix the composite. After thermal curing in a vacuum oven at 80 °C, the composite was cut into 5 μm thick and 6 mm diameter disks with conventional microtome using a quartz blade. The microtome-cut membrane piece was then glued on a polycarbonate plate with a punched hole of 3 mm diameter. The membrane area for permeation was 0.07 cm^2. 15 nm gold (no effect to the membrane permeability) was then sputtered on one side of plate where membrane was glued for applying voltage, which was performed using a Cressington Coating System (Ted-Pella) with a calibrated quartz crystal monitor with background pressure of 0.02 mbar.

Fouling and Defouling of CNT Membranes: Electrophoretic transport of BSA (Sigma) was used to foul CNT membranes. The fouling and electrochemical defouling were performed in a U-tube diffusion filter. For the face-down fouling and defouling experiment, 0.5 mL (≈2 cm high) PBS (consisted of 150 mM NaCl) with a pH corresponding to the protein feed solution was used as permeate solution and ≈7 mL protein solution was filled in other side to keep 3 cm H_2O pressure (Figure 1a). An e-DAQ e-corder 410 potentiostat was used to apply voltage for the electrophoresis fouling. The feed concentration of BSA in pH 7.0 PBS was 2 mg/mL. Two Pt wires used as the counter and working electrodes were respectively set in the feed and permeate sides. The amplitude of electrophoresis voltage was set to be +1 V. After fouling, the membrane was taken out and transferred to another U-tube filter to measure the transmembrane ionic current at the bias of +0.6 V. Two Ag/AgCl solid electrodes (Biomed Products Inc.) that were separately set up in two sides of membrane were utilized to measure the transmembrane ionic current. The measurement duration was 2 min with a 1 point/s data request. The ionic current was averaged to characterize the fouling extent. The electrolyte was 100 mM KCl in DI water and the same height level was kept during the ionic current measurement. For the face-up fouling and defouling experiment, 1 mL (≈4 cm high) protein solution was filled in one side of U-tube filter while ≈4 mL PBS with corresponding pH to protein feed solution was used as permeate as showed in Figure 1b (For vertical setup, ≈3 mL PBS and BSA solution were respectively filled in two tubes separated by the CNT membrane). Two platinum wires were still used as the counter and working electrodes, respectively, for the electrophoresis fouling. Ionic current measurements using two Ag/AgCl solid electrodes and electrochemical defouling were continued without taking the fouled CNT membrane out. For defouling, the CNT membrane was used as the working electrode and Pt wire counter was kept in BSA solution.

The CNT membranes were also fouled using various small molecule solutions, including pyrene butylic acid (0.7 mg/mL in ethanol), naphthalene (10 mg/mL in ethanol), rhodamine B (10 mg/mL in DI water), direct blue dye 71 (10 mg/mL in DI water), Kentucky River water, alginic acid (10 mg/mL in DI water), humic acid (10 mg/mL in DI water), and toluene (10 mg/mL in DI water). Alginic acid and humic acid solutions were adjusted to pH 7 using 1 M concentrated KOH solutions to prevent damaging the membranes (corrosion of polymer matrix) and increase their solubility in aqueous solution. The membrane used was the DWCNT membrane except for the pyrene butylic acid study, in which case the SWCNT membrane was used. To defoul membranes we used a large cation, 50 mM $Ru(bpy)_3^{2+}$ (≈1 nm in diameter) to clean the inner core of nanotubes (molecular brush). Similarly, a U-shape tube with two Ag/AgCl electrodes was employed for the defouling study. The bias applied was –0.9 V. Fouling and defouling durations were determined according to the fouling ability of these foulants. After defouling, the transmembrane ionic current was measured using the U-shape tube as mentioned above.

Membrane Characterization after Electrochemical Treatment: UV-visible spectra were investigated before and after electrochemical oxidation or reduction using SWCNT membrane without BSA fouling. The background of the spectra was a pure microtome-cut epoxy film piece glued on a polycarbonate plate hole without SWCNT loading. SEM images were taken using a Hitachi S-4300 microscope under an operating voltage of 20 kV.

Acknowledgements

This work was supported by NIDA, #5R01DA018822-05, DOE EPSCoR,DE-FG02-07ER46375 and DARPA, W911NF-09-1-0267. Critical infrastructure provided by the University of Kentucky, Center for Nanoscale Science and Engineering.

Received: May 9, 2012
Revised: July 2, 2012
Published online: October 22, 2012

[1] a) A. L. Zydney, *Biotechnol. Bioeng.* **2009**, *103*, 227; b) R. Ghosh, *J. Chromatogr., A* **2002**, *952*, 13; c) J. K. Yuan, X. G. Liu, Q. Akbulut, J. Q. Hu, S. L. Suib, J. Kong, F. Stellacci, *Nat. Nanotechnol.* **2008**, *3*, 332; d) F. Fornasiero, H. G. Park, J. K. Holt, M. Stadermann, C. P. Grigoropoulos, A. Noy, Q. Bakajin, *Proc. Natl. Acad. Sci. USA* **2008**, *105*, 17250; e) C. C. Striemer, T. R. Gaborski, J. L. McGrath, P. M. Fauchet, *Nature* **2007**, *445*, 749.
[2] J. Mansouri, S. Harrisson, V. Chen, *J. Mater. Chem.* **2010**, *20*, 4567.
[3] a) B. J. Hinds, N. Chopra, T. Rantell, R. Andrews, V. Gavalas, L. G. Bachas, *Science* **2004**, *303*, 62; b) M. Majumder, N. Chopra, R. Andrews, B. J. Hinds, *Nature* **2005**, *438*, 44; c) J. K. Holt, H. G. Park, Y. M. Wang, M. Stadermann, A. B. Artyukhin, C. P. Grigoropoulos, A. Noy, O. Bakajin, *Science* **2006**, *312*, 1034.
[4] a) M. Majumder, N. Chopra, B. J. Hinds, *J. Am. Chem. Soc.* **2005**, *127*, 9062; b) B. J. Hinds, *Curr. Opin. Solid State Mater. Sci.* **2012**, *16*, 1.
[5] a) J. Wu, K. Gerstandt, M. Majumder, X. Zhan, B. J. Hinds, *Nanoscale* **2011**, *3*, 3321; b) J. Wu, K. Gerstandt, H. B. Zhang, J. Liu, B. J. Hinds, *Nat. Nanotechnol.* **2012**, *7*, 133; c) P. Pang, J. He, J. H. Park, P. S. Krstic, S. Lindsay, *ACS Nano* **2011**, *5*, 7277.
[6] X. J. Gong, J. C. Li, K. Xu, J. F. Wang, H. Yang, *J. Am. Chem. Soc.* **2010**, *132*, 1873.
[7] J. Wu, K. S. Paudel, C. Strasinger, D. Hammell, A. L. Stinchcomb, B. J. Hinds, *Proc. Natl. Acad. Sci. USA* **2010**, *107*, 11698.
[8] X. H. Sun, X. Su, J. Wu, B. J. Hinds, *Langmuir* **2011**, *27*, 3150.
[9] a) D. M. Kanani, X. H. Sun, R. Ghosh, *J. Membr. Sci.* **2008**, *315*, 1; b) X. H. Sun, D. M. Kanani, R. Ghosh, *J. Membr. Sci.* **2008**, *320*, 372; c) R. Chan, V. Chen, *J. Membr. Sci.* **2004**, *242*, 169; d) C. Duclos-Orsello, W. Y. Li, C. C. Ho, *J. Membr. Sci.* **2006**, *280*, 856; e) C. C. Ho, A. L. Zydney, *J. Colloid Interface Sci.* **2000**, *232*, 389; f) G. Belfort, R. H. Davis, A. L. Zydney, *J. Membr. Sci.* **1994**, *96*, 1; g) R. W. Field, D. Wu, J. A. Howell, B. B. Gupta, *J. Membr. Sci.* **1995**, *100*, 259; h) S. K. Hong, M. Elimelech, *J. Membr. Sci.* **1997**, *132*, 159; i) W. H. Peng, I. C. Escobar, D. B. White, *J. Membr. Sci.* **2004**, *238*, 33.
[10] Z. G. Mao, S. B. Sinnott, *J. Phys. Chem. B* **2000**, *104*, 4618.
[11] a) M. Majumder, X. Zhan, R. Andrews, B. J. Hinds, *Langmuir* **2007**, *23*, 8624; b) X. Su, J. Wu, B. J. Hinds, *Carbon* **2011**, *49*, 1145.
[12] a) T. Ito, L. Sun, R. M. Crooks, *Electrochem. Solid-State Lett.* **2003**, *6*, C4; b) D. C. Wei, Y. Q. Liu, L. C. Cao, H. L. Zhang, L. P. Huang, G. Yu, H. Kajiura, Y. M. Li, *Adv. Funct. Mater.* **2009**, *19*, 3618.
[13] A. Agarwal, W. J. Ng, Y. Liu, *Chemosphere* **2011**, *84*, 1175.
[14] a) M. Chiku, T. A. Ivandini, A. Kamiya, A. Fujishima, Y. Einaga, *J. Electroanal. Chem.* **2008**, *612*, 201; b) M. Chiku, J. Nakamura, A. Fujishima, Y. Einaga, *Anal. Chem.* **2008**, *80*, 5783.
[15] X. H. Sun, Z. D. Chang, S. F. Shen, X. Hu, H. Z. Liu, *Colloids Surf., A* **2006**, *286*, 8.
[16] Y. C. Zhu, G. J. Cheng, S. J. Dong, *Biophys. Chem.* **2001**, *90*, 1.
[17] J. Wu, X. Zhan, B. J. Hinds, *Chem. Commun.* **2012**, *48*, 7979.
[18] R. Andrews, D. Jacques, A. M. Rao, F. Derbyshire, D. Qian, X. Fan, E. C. Dickey, J. Chen, *Chem. Phys. Lett.* **1999**, *303*, 467.
[19] L. Sun, R. M. Crooks, *J. Am. Chem. Soc.* **2000**, *122*, 12340.